Anion Exchange Ionomers Enable Sustained Pure-Water Electrolysis using Platinum-group-metal-free Electrocatalysts

*Yiwei Zheng[1], Ariana Serban[1], Haoyue Zhang[2], Nanjun Chen[1], Fang Song[2] and Xile Hu[1]**

[1]Laboratory of Inorganic Synthesis and Catalysis

Institute of Chemical Sciences and Engineering

Ecole Polytechnique Fédérale de Lausanne (EPFL)

Lausanne CH-1015, Switzerland

[2]State Key Lab of Metal Matrix Composites

School of Materials Science and Engineering

Shanghai Jiao Tong University (SJTU)

800 Dongchuan Rd., Minhang District, Shanghai 200240, China

Corresponding Author

* Email: xile.hu@epfl.ch

ABSTRACT Anion exchange membrane water electrolyzer (AEMWE) is a rising technology that offers potential advantages in cost and scalability over proton exchange membrane water electrolyzer (PEMWE) technology. However, AEMWEs that stably operate in pure water still employ platinum-group-metal (PGM) catalysts, especially at the cathode. Here, by using an appropriate ionomer at both anode and cathode, as well as a new hydrogen evolution reaction (HER) catalyst, we achieve sustained pure-water AEM water electrolysis using only PGM-free electrocatalysts. Our optimized AEMWE can operate stably for more than 550 h at 1 A/cm^2 with a cell voltage of 1.82 V. This performance competes favorably over the state-of-the-art, PGM-containing, AEMWEs. Unexpectedly, we find that the cathode performance is the bottleneck in pure-water AEMWE. The application of a cathode ionomer can lower the cell voltage by up to 1.4 V at 1 A/cm^2. Our work reveals the importance of ionomers for pure-water AEMWEs and identifies cathode improvement as a key area for future work.

TOC GRAPHICS

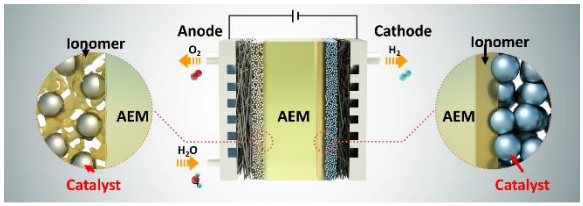

To combine the advantages of alkaline water electrolysis (AWE) and proton exchange membrane water electrolysis (PEMWE), a considerable amount of time and effort have been devoted over the last decade to the development of the technology known as anion exchange membrane water electrolysis (AEMWE). Recently, AEMWE's performance and stability have been enhanced to the point where their future deployment in real applications can be seriously considered. For example, AEMWEs' cell voltage is reported to be as low as 1.55 ~ 1.7 V at 1 A/cm^2 operating in 1.0 M KOH.[1–6] In addition, multiple groups have reported 500+ h stability in 1.0 M KOH at low degradation rates[2,5,6] and one recent study showed durability over 8900 h for a 50 cm^2 AEMWE at 200 mA/cm^2.[7] The best-reported stability was obtained by Motealleh et al.[8], whose electrolyzer worked in 1.0 M KOH at 1 A/cm^2 for 11000+ h with a degradation rate of 0.7 μV/h.

Despite the rapid development of AEMWE technology operating in alkaline electrolyte, AEMWE should be operated in a pure water-fed condition ultimately. Pure water instead of an alkaline electrolyte, typically 1.0 M KOH, which is corrosive, means a simpler balance of plant (BOP), less passivation for bipolar plates, and no shunt currents. All these translate into a low cost. There are only a few attempts on developing stable pure-water-fed AEMWE.[1,5,9–16] For example, an AEMWE based on PiperION membrane and PGM catalysts operated for over 175 h with a degradation rate of 0.67 mV/h.[17] Likewise Hassan et al.[5] used platinum-nickel and iridium oxide as HER and oxygen evolution reaction (OER) catalysts for AEMWE pure water operation at the current density of 1.0 A/cm^2 for 500 h at an operating voltage of ca. 2 V and a low degradation rate. Li et al.[1] developed an ammonium-enriched AEI to improve the pure water AEMWE performance with the use of NiFe-based OER catalyst and PtRu/C HER catalyst. However, this cell showed a large deviation from its transient performance during the stability test at 200 mA/cm^2. Wan et al.[18] employed vertically aligned ionomer-incorporated FeNi layered

double hydroxide (LDH) nanosheet arrays OER catalyst and Pt/C HER catalyst to achieve stability of 180 h at 500 mA/cm^2. In all these cases, Pt/C is employed as the HER catalyst. Thus, although one of the biggest advantages of AEMWE technology is the possibility to use PGM-free catalysts, this advantage has not been demonstrated in pure-water AEMWE, largely due to the lack of suitable PGM-free HER catalysts. Additionally, the impact of ionomer on AEM electrolyser performance is less studied, although some reports indicate their important roles. For example, Li et al.[1] designed an ionomer with no phenyl groups from the polymer backbone to create a high local pH for efficient HER and OER. Chen et al.[11] showed that ionomer swelling is more critical than membrane swelling for AEMWE stability and reduction of ionomer swelling could enhance the lifetime of pure-water-fed AEMWEs.

In this study, we have developed stable pure-water AEMWEs using PGM-free OER and HER catalysts. We show that with the aid of appropriate ionomers, AEMWE performance and stability in pure water can be greatly enhanced. Our analysis reveals cathode performance as the main performance bottleneck in PGM-free AEMWEs.

Catalysts and electrodes

Two representatives of PGM and PGM-free OER catalysts (IrO_2 and NiFe-based catalysts) were used in this work. For PGM-free catalyst, both self-supported and powdery formats were synthesized. The method for self-supported PGM-free catalyst NiFeOOH has been reported[19]. The powdery NiFeOOH was prepared following a new procedure (see the Supporting Information). Powdery catalysts were made into catalyst ink and then sprayed onto Ni felt porous transport layer (PTL). Both PGM and PGM-free cathodes were used, including spray coated

powdery Pt/C and a new electrodeposited, self-supported NiMo on Toray TGP-H-060 PTL (C papers), respectively. The details of the latter can be found in the Supporting Information.

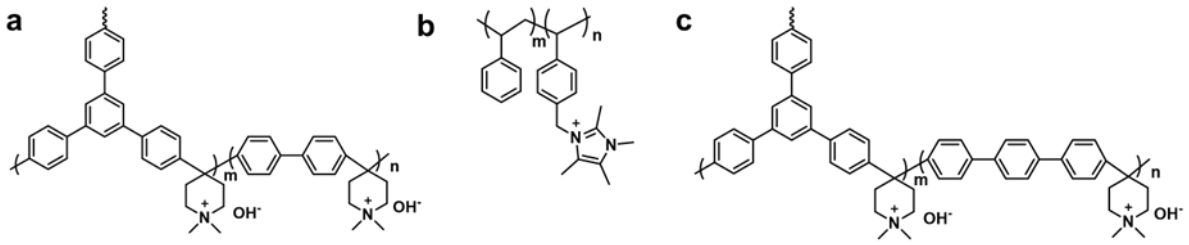

Figure 1. Chemical structure of a) branched poly(biphenyl piperidinium) (b-PBP) ionomer; b) Sustainion XB-7; c) branched poly(terphenyl piperidinium) (b-PTP) AEM.

The AEIs are branched poly(biphenyl piperidinium) ionomer (b-PBP)[20] (Branion by NovaMea) with an ion exchange capacity (IEC) of 3.4 mmol/g (Figure 1 a) and XB-7 (Sustainion by Dioxide Materials, IEC = 2.2 mmol/g, Figure 1b). 25 μm branched poly(terphenyl piperidinium) AEM (Branion by NovaMea) with 1 mol% of 1,3,5-triphenylbenzene comonomer (b-PTP-1, IEC = 2.81 mmol/g) was used in this study for performance test (Figure 1c).[20]

Electrocatalytic performance in three-electrode cells

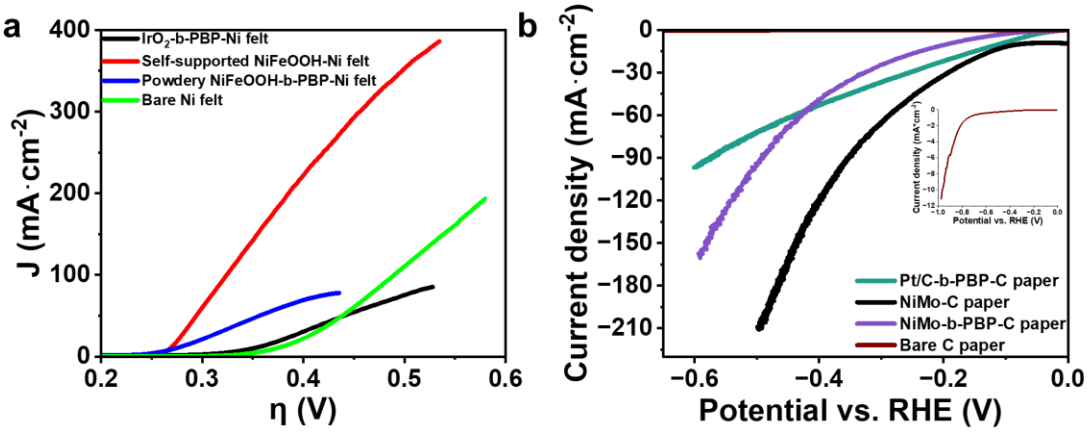

Figure 2. a) OER polarization curves in 1.0 M KOH; b) HER polarization curves tested in 1.0 M KOH, inset: LSV curves of bare carbon paper.

Electrode materials assembled in AEMWE (SEM images shown in Figure S1) were first tested in a three-electrode setup for LSV and C_{dl} measurements. In Figure 2a, the benchmark PGM OER catalyst IrO_2 shows the highest overpotential of 0.57 V at 100 mA/cm^2 in 1.0 M KOH at 25 ºC, while the self-supported NiFeOOH-Ni felt catalyst has the lowest overpotential of 0.32 V. The spray-coated powdery NiFeOOH-b-PBP-Ni felt is less active than self-supported NiFeOOH due to a lower catalyst loading and the presence of b-PBP ionomer which blocks some of the active sites. Note that as an ionomer is needed to bind catalyst particles to electrodes, the presence of ionomers cannot be avoided for powdery catalysts. The HER catalytic performance is shown in Figure 2b. NiMo grown on carbon paper exhibits the best HER activity, reaching 100 mA/cm^2 at 0.35 V vs. RHE, which is better than the benchmark PGM catalyst of Pt/C sprayed on carbon paper (0.58 $V_{vs.\ RHE}$ at 100 mA/cm^2). The latter contains b-PBP ionomer that is required to bind the catalyst to the electrode. Coating NiMo-C paper with b-PBP ionomer decreased the HER activity (0.49 $V_{vs.\ RHE}$ at 100 mA/cm^2), which can be attributed to ionomer-induced electronic insulation and a decreased ECSA (Table S1, derived from C_{dl} in Figure S2). The ECSA-normalized LSVs arepresented in Figure S3. According to the data above, the NiFeOOH and NiMo catalysts described here exhibit higher activity than benchmark PGM catalysts in three-electrode cells. XRD patterns of NiMo-C paper and NiMo-b-PBP-C paper in Figure S4 show no phase changes after ionomer coating.

Critical influence of ionomers in PGM-free AEMWE

In three-electrode experiments, the reactions are conducted in 1.0 M KOH. The KOH permeates the porous catalyst assembly in ways that the solid ionomer cannot. Therefore, membrane-electrode-assembly (MEA) results are not always consistent with three-electrode behaviors and the deviations are mainly due to catalyst utilization, mass transport limitations (electrolyte access

and bubble removal), and ionic and electrical conductivity. Thus, after testing in three-electrode setup, the catalysts are tested in alkaline and pure water-fed two-electrode AEMWEs. The MEAs were loaded into 4 cm^2 Scribner hardware between single-pass serpentine flow nickel and graphite plates. b-PTP, nickel felt and carbon paper are used as as AEM, anode and cathode substrates, respectively.

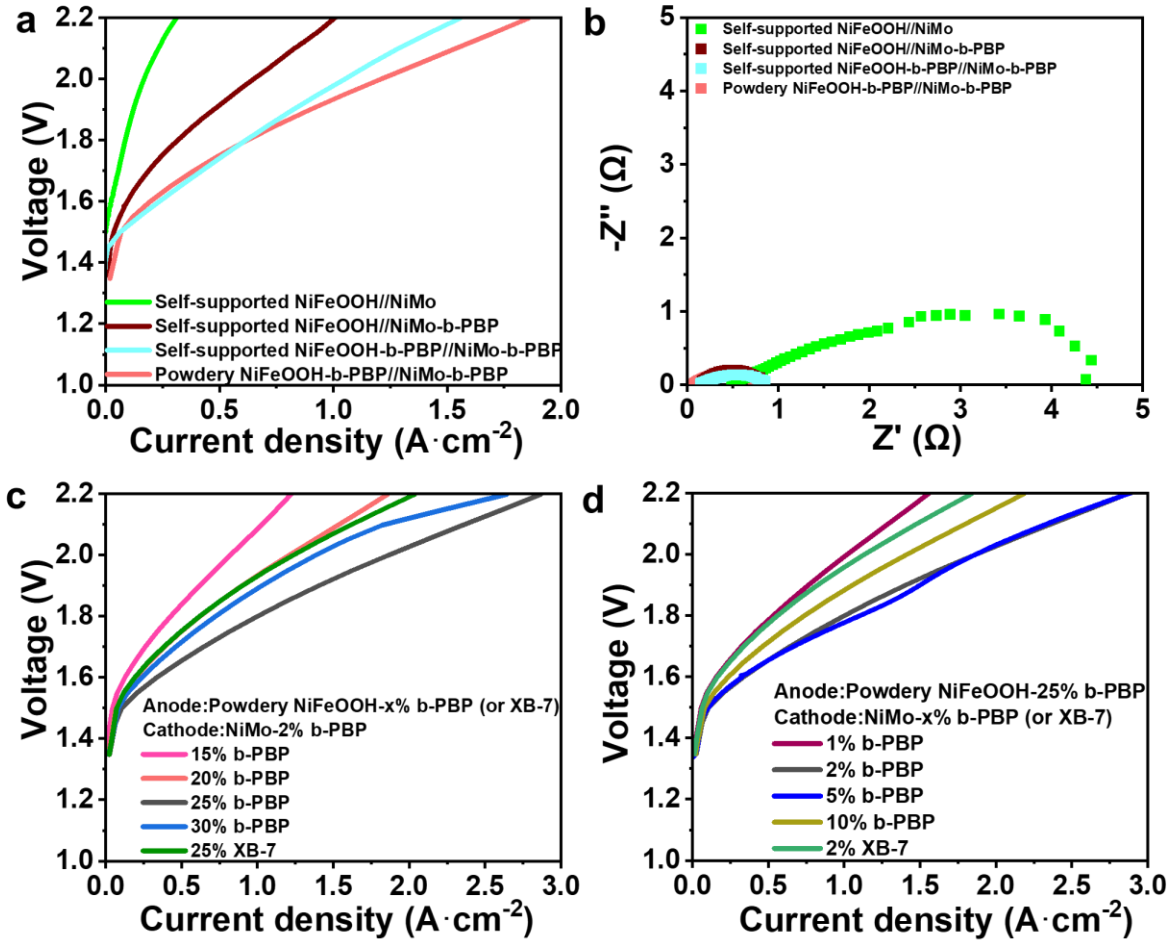

Figure 3. a) polarization curves of pure water-fed PGM-free AEMWEs showing the influences of ionomers (anode: self-supported and powdery NiFeOOH have 5 % (to total catalyst mass) and 20 wt% (to total catalyst layer mass) b-PBP, respectively; cathode: 2 wt% b-PBP); b) corresponding EIS measurements at 0.1 A/cm^2; c) polarization curves of pure water-fed PGM-free AEMWEs w/ ionomer, anode ionomer contents vary from 15 wt% to 30 wt%, cathode ionomer was kept at 2 wt% (XB-7 with smaller IEC for 25 wt% case only); d) polarization curves of pure water-fed PGM-free AEMWEs w/ ionomer, anode ionomer was kept at 25 wt%,

cathode ionomer was changing from 1 wt% to 10 wt% (XB-7 for 2 wt% case only). Cell and electrolyte temperatures at 80 °C.

At first, we tested the influences of ionomers for PGM-free catalysts in pure water AEMWEs. Figure 3 a) shows that adding b-PBP ionomer to the NiMo-C paper cathode increases the performance of the AEMWE with a self-supported NiFeOOH//NiMo electrode pair. The current density at 2.0 V is increased from 0.17 to 0.66 A/cm^2. Adding b-PBP ionomer to self-supported NiFeOOH anode further increases the performance. The current density at 2.0 V is now 1.05 A/cm^2. Replacing the self-supported NiFeOOH-b-PBP with powdery NiFeOOH-b-PBP yields even higher performance, resulting in a current density of 1.21 A/cm^2 at 2.0 V. These results suggest both cathode and anode ionomers greatly improved the full-cell performance of pure water AEMWEs. Due to being ionomer-free, the active sites of self−supported NiFeOOH are able to full contact with electrolyte, thus, self−supported NiFeOOH achieves the highest performance in three-electrode cell. However, the conclusion in three-electrode test cannot be transferred to a two-electrode electrolyser. The addition of ionomer on electrode (self−supported NiFeOOH−b−PBP (blue line) and powdery NiFeOOH−b−PBP (pink line)) has greatly improved the electrolyser performance because of better hydroxide conduction.

EIS curves in Figure 3 b show that the ionomer-free self-supported NiFeOOH//NiMo pair stands out for the largest resistance due to the low electrical conductivity of electrocatalysts and the lack of OH^- conducting channel. Ionomer coating has largely reduced interfacial contact resistance between the electrode and the membrane. Moreover, the apparent charge-transfer resistance, which includes both kinetic and mass transfer terms, largely decreases with the application of ionomers. This can be attributed to the ionomer functioning as an OH^- buffer layer to facilitate the transport of OH^- ions, then improving the OER and HER for pure-water-fed AEMWE.

We next probed the influence of ionomer contents (Figure 3 c and d). For the anode, when b-PBP is used as ionomer, increasing its content first increases its performance, until the best results were obtained at 25 wt%. A higher content led to lower performance, possibly because a large amount of ionomer can block some active sites, as well as decrease electronic conductivity. We also compared b-PBP and XB-7 as anode ionomers at 25 wt% loading and found b-PBP worked better. We attribute this to the higher IEC of b-PBP (3.4 mmol/g) compared to XB-7 (2.2 mmol/g), which is more efficient for hydroxide transfer.

The anode ionomer was then kept at 25 wt% b-PBP, and the content of b-PBP in the cathode was changed from 1 to 10 wt%. It was found that 2 wt% and 5 wt% ionomer content was the best. We also compared b-PBP and XB-7 as cathode ionomers at 2 wt% loading, and the b-PBP was again better, possibly due to a higher IEC as well. The effect of ionomer comes partially from the accessibility of catalyst active sites to hydroxide. The higher loading of ionomer naturally reduces the amount of accessible hydroxide ions while appropriate amount of ionomer could enhance hydroxide tranport.

As a reference, we probed the influences of ionomers for AEMWEs working with 1.0 M KOH as anode electrolyte (Figure S5). Only at current densities higher than 2 A/cm^2, ionomers have a noticeable, positive influence on the performance. The degree of improvement is however modest compared to that in pure water AEMWEs. This result can be understood considering a more hydroxide-rich environment when 1.0 M KOH is used as anode electrolyte. In accordance with this, the content of anode ionomer, as well as the nature of ionomer (b-PBP or XB-7), made little to small differences (Figure S5 c and d)

Comparison of PGM-free AEMWEs with PGM-containing AEMWEs

We next compared AEMWEs with PGM//PGM, PGM-free//PGM, and PGM-free//PGM-free (anode//cathode) electrode configurations (Figure 4). For the PGM-free electrodes, we chose the best pair from the study in Figure 3. In pure water, the PGM (IrO_2-b-PBP)//PGM (Pt/C-b-PBP) combination gave the worst result, whereas the powdery NiFeOOH-b-PBP//NiMo-b-PBP had the same performance as NiFeOOH-b-PBP//Pt/C-b-PBP (Figure 4a). It can be concluded that the powdery NiFeOOH is much better than IrO_2 for OER, and the NiMo is similar to Pt/C for HER in pure-water AEMWEs. The electrolyser performance of IrO_2 MEA is comparable to those reported in reference.[5,21,22] Figure 4b compares the state-of-the-art pure-water AEMWEs. Our PGM-free AEMWE has the highest performance of 1.91 A/cm^2 at 2.0 V. Figure 4c shows that the AEMWE with powdery NiFeOOH-b-PBP//NiMo-b-PBP can be stably operated for more than 550 h at 1 A/cm^2. The voltage is at around 1.82 V, with a degradation rate of 71 μV/h. Combine with optimized testing system and materials - the optimized electrodes contain high-performant catalysts and optimized ionomer coating as well as the high durability of AEM proven by our previous publications[20,23,24], such high performance and stability was achieved. Post mortem analysis in Figure S7 shows that after 550 h of stability test the LSV performance has decreased from the prestine sample due to an increase in ohmic and charge transfer resistances. SEM images show that the anode morphology has changed while that of the cathode remains similar after electrolysis. Likewise, XRD patterns show that the anode catalyst becomes more amorphous whereas the cathode catalyst retains its structure after electrolysis. These results suggest that the decrease of MEA performance is mostly due to the change of the anode catalyst, possibly due to phase change or detachment.

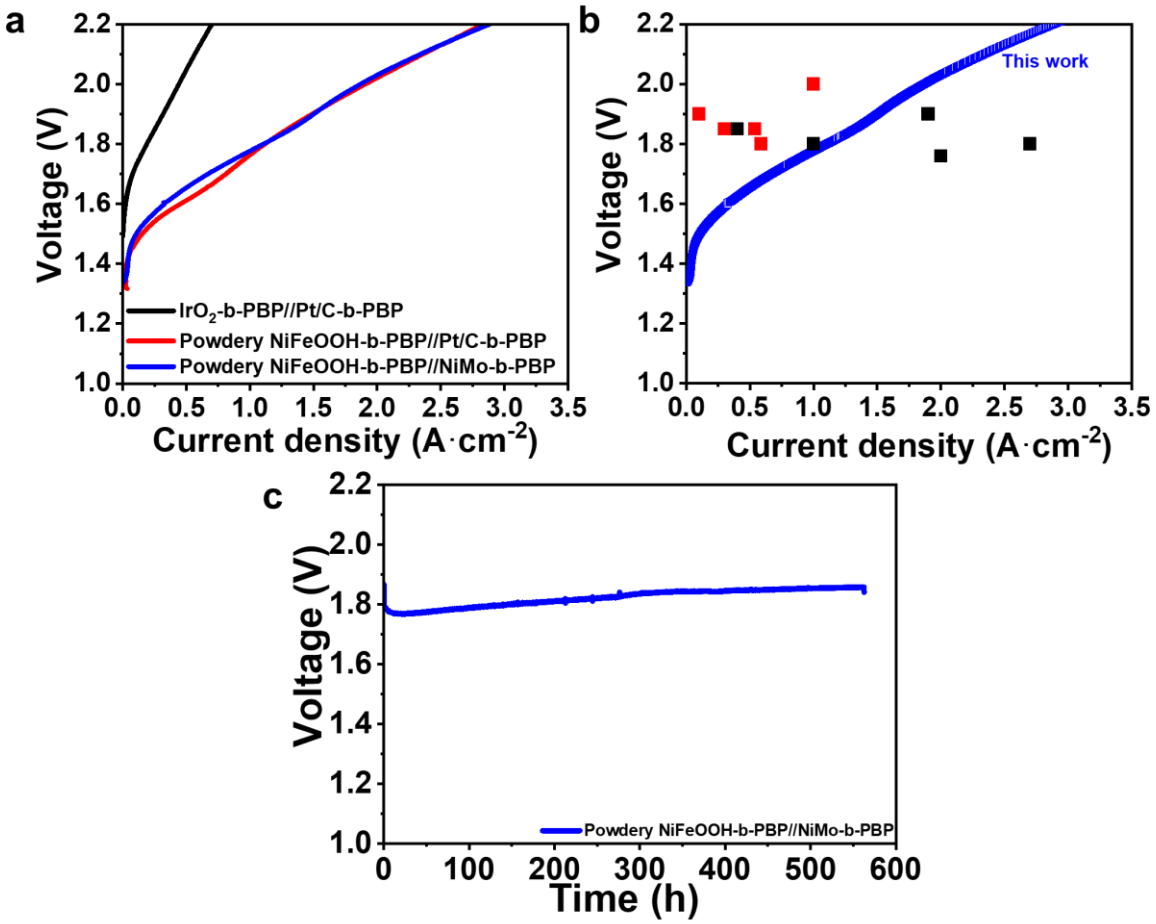

Figure 4. a) polarization curves of PGM//PGM, PGM-free//PGM, and PGM-free//PGM-free AEMWEs in pure water; b) AEMWE performance collection in pure water from reference, red dots for PGM-free cells, black dots for PGM-contained cells;[9,12,15,25] c) stability at a constant current density of 1 A/cm^2. Cell and electrolyte temperatures at 80 ºC. The PGM-free cell is the same blue curve in Figure 3 d).

Analysis of performance-determining factors

We conducted EIS analysis and fitted polarization curves to trace the performance loss sources of various pure water AEMWEs presented here. The ohmic loss was taken from Galvano-EIS measurement. The kinetics overpotential was determined by fitting a Tafel model to the Ohmic loss-free overpotential below 30 mA/cm^2. The mass transport overpotential was determined by subtracting the kinetics overpotential from the iR-free overpotential (see

corresponding formulas in SI). Figure 5a shows the contributions of each mechanism at the current densities of 0.1 and 0.5 A/cm^2. As expected, increasing the current density often leads to higher mass transfer overpotentials, but not for the powdery NiFeOOH-b-PBP//Pt/C-b-PBP. In the latter case, there is nearly no mass transfer overpotential, highlighting the efficiency of both its cathode and anode ionomers. For this pair, most loss is due to kinetic overpotential. Interestingly, the kinetic overpotentials are the lowest for the NiFeOOH-b-PBP//NiMo-b-PBP pair, indicating the NiMo catalyst has a higher intrinsic activity than Pt/C. This result is consistent with that of the three-electrode measurements (Figure 2b). For the NiFeOOH-b-PBP//NiMo-b-PBP pair, a large portion of the loss is due to mass transfer resistance, and mostly from the cathode. For reference, data for AEMWEs running in 1.0 M KOH are shown in Figure S6. Again a large difference in performance profiles is observed between AEMWEs running in 1.0 M KOH and those in pure water, due to the change of electrolyte environment.

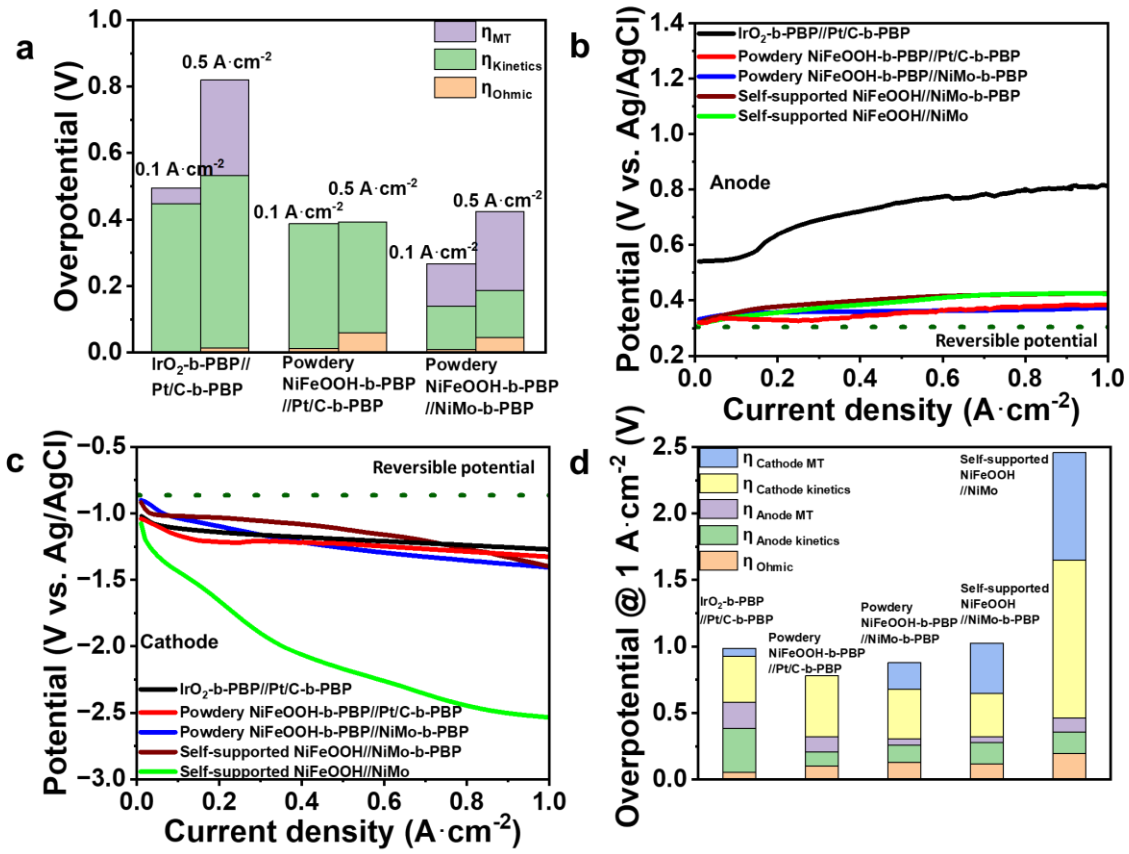

Figure 5. a) performance loss distribution in water at 0.1 and 0.5 A/cm^2 (derived from Figure 4a); b) and c) for anode and cathode iR- corrected potentials of AEMWEs in pure water; d) overpotential breakdowns. Sustainion X37-50 grade T AEM for b), c), and d). Cell and electrolyte temperatures at 80 ºC.

To obtain further details of the voltage losses, we used an extended AEM strip out of hardware with an Ag/AgCl reference electrode to identify the potential for each electrode (Figure S8).[26] EIS measurements were done between the reference electrode and the anode or cathode (Figure S11), and the recorded potentials were corrected by the Ohmic resistance extracted from the corresponding EIS curves. The I-V curves obtained in this system (Figure S9) are similar in trend to those recorded in normal cells (Figures 3 and 4), even though a different AEM and active area of the cell was used in the present case. The iR-corrected net potential losses at the anode and cathode are shown in Figures 5b and c. For the anode, IrO_2-b-PBP is clearly much less efficient

than NiFeOOH-based electrodes. Among the latter, powdery NiFeOOH-b-PBP has the lowest anode potential, consistent with cell data in Figure 3a. For the cathode, ionomer-free NiMo-C paper has very negative potentials, but the coating of this catalyst with 5 wt% b-PBP greatly improved the cathode performance, for example, by about 1.4 V at 1 A/cm^2.

We further break down the overpotentials into mass transfer and kinetic overpotentials. Figure 5d compares the contributions of various loss mechanisms for different AEMWEs at 1 A/cm^2. Ohmic loss is negligible for IrO_2-b-PBP//Pt/C-b-PBP, due to the high conductivity of PGMs. The use of less conductive PGM-free catalysts resulted in a small Ohmic loss. Surprisingly, in all cases, the cathode kinetic overpotential is the biggest contributor to the overall cell voltage, even for Pt/C. When NiFeOOH catalysts are used, the anode overpotential loss is rather small. These data are in contrast to the general assumption that OER rather than HER is the bottleneck in water splitting. We think this result arises from the particular environment of pure-water AEMWEs, which is rather different from three-electrode cells where mass transport is often not an issue. This could also come from relatively lower local pH in cathode/membrane interface in pure water-fed working environment than in alkaline media. A lower pH could decelerate the intrinsic activity of HER catalyst. The importance of OH^- transport at the cathode is highlighted by the massive reduction of potential (1.4 V) upon application of a small amount of b-PBP to the cathode. As expected, in AEMWEs operating with 1.0 M KOH anolyte, mass transfer overpotentials are greatly reduced, and kinetics are even slightly improved (Figure S10). The huge influence of cathode ionomer nearly vanishes, consistent with the abundant OH^- provided by the anolyte, likely via cross-over through the membrane. Continuously in all cases, cathode kinetic overpotential is the biggest contributor to the cell voltage.

We have demonstrated sustained pure-water AEM water electrolysis using PGM-free electrocatalyst. We have shown that such PGM-free AEMWEs perform as good as or better than state-of-the-art PGM-containing AEMWEs under similar conditions. Our optimized AEMWE can operate stably for more than 550 h at 1 A/cm^2 with a cell voltage of 1.82 V. We show that an appropriate ionomer at both the anode and cathode is essential for a high-performance pure-water AEMWE. The application of a cathode ionomer can lower the cell voltage by up to 1.4 V at 1 A/cm^2. Unexpectedly, we find that the cathode performance is the bottleneck in pure-water AEMWE. Future work in improving the performance of pure-water AEMWEs should focus on the cathode.

AUTHOR INFORMATION

Corresponding Author: Xile Hu, Email: xile.hu@epfl.ch

Notes

A.S and X.L. Hu are inventors of a patent application that includes the HER catalyst used in this paper. The branched PAP AEM used in this work is commercialized under the brand name "Branion" by an EPFL Startup NovaMea SA, of which N.J.Chen, F.Song, and X.L. Hu have a financial interest.

SUPPORTING INFORMATION

Electrochemical measurements: C_{dl}, LSV, ECSA; physicochemical analysis: SEM, XRD; additional polarization curves, stabilities, EIS measurements.

ACKNOWLEDGMENT

The authors from EPFL gratefully acknowledge the financial support of the GazNat SA, the EPFL, and the Valais Energy Demonstrators project AMY. The authors from SJTU acknowledge the support from Shanghai Science and Technology Committee (Grant Nos. 23ZR1433000) and the National High-Level Talent Program for Young Scholars (for F.S.). We thank Dr. Wenchao Ma (EPFL) for SEM characterization and Ms. Yang Liu for the design of TOC image.

REFERENCES

(1) Li, D.; Park, E. J.; Zhu, W.; Shi, Q.; Zhou, Y.; Tian, H.; Lin, Y.; Serov, A.; Zulevi, B.; Baca, E. D.; Fujimoto, C.; Chung, H. T.; Kim, Y. S. Highly Quaternized Polystyrene Ionomers for High Performance Anion Exchange Membrane Water Electrolysers. *Nat Energy* **2020**, *5* (5), 378–385. https://doi.org/10.1038/s41560-020-0577-x.

(2) Chen, N.; Sae, Y.; Ju, Y.; Jong, H.; So, Y.; Young, M. High-Performance Anion Exchange Membrane Water Electrolyzers with a Current Density of 7.68 A Cm −2 and a Durability of 1000 Hours. *Energy & Environmental Science* **2021**, *14* (12), 6338–6348. https://doi.org/10.1039/D1EE02642A.

(3) Kang, S. Y.; Park, J. E.; Jang, G. Y.; Kim, O.-H.; Kwon, O. J.; Cho, Y.-H.; Sung, Y.-E. High-Performance and Durable Water Electrolysis Using a Highly Conductive and Stable Anion-Exchange Membrane. *International Journal of Hydrogen Energy* **2022**, *47* (15), 9115–9126. https://doi.org/10.1016/j.ijhydene.2022.01.002.

(4) Sankar, S.; Roby, S.; Kuroki, H.; Miyanishi, S.; Tamaki, T.; Anilkumar, G. M.; Yamaguchi, T. High-Performing Anion Exchange Membrane Water Electrolysis Using Self-Supported Metal Phosphide Anode Catalysts and an Ether-Free Aromatic Polyelectrolyte. *ACS Sustainable Chem. Eng.* **2023**, *11* (3), 854–865. https://doi.org/10.1021/acssuschemeng.2c03663.

(5) Hassan, N. U.; Zheng, Y.; Kohl, P. A.; Mustain, W. E. KOH vs Deionized Water Operation in Anion Exchange Membrane Electrolyzers. *J. Electrochem. Soc.* **2022**, *169* (4), 044526. https://doi.org/10.1149/1945-7111/ac5f1d.

(6) Hassan, N. U.; Mandal, M.; Zulevi, B.; Kohl, P. A.; Mustain, W. E. Understanding and Improving Anode Performance in an Alkaline Membrane Electrolyzer Using Statistical Design of Experiments. *Electrochimica Acta* **2022**, *409*, 140001. https://doi.org/10.1016/j.electacta.2022.140001.

(7) Moreno-González, M.; Mardle, P.; Zhu, S.; Gholamkhass, B.; Jones, S.; Chen, N.; Britton, B.; Holdcroft, S. One Year Operation of an Anion Exchange Membrane Water Electrolyzer Utilizing Aemion+® Membrane: Minimal Degradation, Low H2 Crossover and High Efficiency. *Journal of Power Sources Advances* **2023**, *19*, 100109. https://doi.org/10.1016/j.powera.2023.100109.

(8) Motealleh, B.; Liu, Z.; Masel, R. I.; Sculley, J. P.; Richard Ni, Z.; Meroueh, L. Next-Generation Anion Exchange Membrane Water Electrolyzers Operating for Commercially

Relevant Lifetimes. *International Journal of Hydrogen Energy* **2021**, *46* (5), 3379–3386. https://doi.org/10.1016/j.ijhydene.2020.10.244.

(9) Wu, X.; Scott, K. A Polymethacrylate-Based Quaternary Ammonium OH− Ionomer Binder for Non-Precious Metal Alkaline Anion Exchange Membrane Water Electrolysers. *Journal of Power Sources* **2012**, *214*, 124–129. https://doi.org/10.1016/j.jpowsour.2012.03.069.

(10) Razmjooei, F.; Morawietz, T.; Taghizadeh, E.; Hadjixenophontos, E.; Mues, L.; Gerle, M.; Wood, B. D.; Harms, C.; Gago, A. S.; Ansar, S. A.; Friedrich, K. A. Increasing the Performance of an Anion-Exchange Membrane Electrolyzer Operating in Pure Water with a Nickel-Based Microporous Layer. *Joule* **2021**, *5* (7), 1776–1799. https://doi.org/10.1016/j.joule.2021.05.006.

(11) Chen, B.; Mardle, P.; Holdcroft, S. Probing the Effect of Ionomer Swelling on the Stability of Anion Exchange Membrane Water Electrolyzers. *Journal of Power Sources* **2022**, *550*, 232134. https://doi.org/10.1016/j.jpowsour.2022.232134.

(12) Xiao, L.; Zhang, S.; Pan, J.; Yang, C.; He, M.; Zhuang, L.; Lu, J. First Implementation of Alkaline Polymer Electrolyte Water Electrolysis Working Only with Pure Water. *Energy Environ. Sci.* **2012**, *5* (7), 7869–7871. https://doi.org/10.1039/C2EE22146B.

(13) Lei, C.; Yang, K.; Wang, G.; Wang, G.; Lu, J.; Xiao, L.; Zhuang, L. Impact of Catalyst Reconstruction on the Durability of Anion Exchange Membrane Water Electrolysis. *ACS Sustainable Chem. Eng.* **2022**, *10* (50), 16725–16733. https://doi.org/10.1021/acssuschemeng.2c04855.

(14) Parrondo, J.; Arges, C. G.; Niedzwiecki, M.; Anderson, E. B.; Ayers, K. E.; Ramani, V. Degradation of Anion Exchange Membranes Used for Hydrogen Production by Ultrapure Water Electrolysis. *RSC Adv.* **2014**, *4* (19), 9875–9879. https://doi.org/10.1039/C3RA46630B.

(15) Thangavel, P.; Ha, M.; Kumaraguru, S.; Meena, A.; Singh, A. N.; Harzandi, A. M.; Kim, K. S. Graphene-Nanoplatelets-Supported NiFe-MOF: High-Efficiency and Ultra-Stable Oxygen Electrodes for Sustained Alkaline Anion Exchange Membrane Water Electrolysis. *Energy Environ. Sci.* **2020**, *13* (10), 3447–3458. https://doi.org/10.1039/D0EE00877J.

(16) Yang, J.; Jang, M. J.; Zeng, X.; Park, Y. S.; Lee, J.; Choi, S. M.; Yin, Y. Non-Precious Electrocatalysts for Oxygen Evolution Reaction in Anion Exchange Membrane Water Electrolysis: A Mini Review. *Electrochemistry Communications* **2021**, *131*, 107118. https://doi.org/10.1016/j.elecom.2021.107118.

(17) Xiao, J.; Oliveira, A. M.; Wang, L.; Zhao, Y.; Wang, T.; Wang, J.; Setzler, B. P.; Yan, Y. Water-Fed Hydroxide Exchange Membrane Electrolyzer Enabled by a Fluoride-Incorporated Nickel–Iron Oxyhydroxide Oxygen Evolution Electrode. *ACS Catal.* **2021**, *11* (1), 264–270. https://doi.org/10.1021/acscatal.0c04200.

(18) Wan, L.; Liu, J.; Xu, Z.; Xu, Q.; Pang, M.; Wang, P.; Wang, B. Construction of Integrated Electrodes with Transport Highways for Pure-Water-Fed Anion Exchange Membrane Water Electrolysis. *Small* **2022**, *18* (21), 2200380. https://doi.org/10.1002/smll.202200380.

(19) Zhang, Y.; Guo, P.; Niu, S.; Wu, J.; Wang, W.; Song, B.; Wang, X.; Jiang, Z.; Xu, P. Magnetic Field Enhanced Electrocatalytic Oxygen Evolution of NiFe-LDH/Co3O4 p-n Heterojunction Supported on Nickel Foam. *Small Methods* **2022**, *6* (6), 2200084. https://doi.org/10.1002/smtd.202200084.

(20) Wu, X.; Chen, N.; Klok, H.-A.; Lee, Y. M.; Hu, X. Branched Poly(Aryl Piperidinium) Membranes for Anion-Exchange Membrane Fuel Cells. *Angewandte Chemie International Edition* **2022**, *61* (7), e202114892. https://doi.org/10.1002/anie.202114892.

(21) Krivina, R. A.; Ou, Y.; Xu, Q.; Twight, L. P.; Stovall, T. N.; Boettcher, S. W. Oxygen Electrocatalysis on Mixed-Metal Oxides/Oxyhydroxides: From Fundamentals to Membrane Electrolyzer Technology. *Acc. Mater. Res.* **2021**, *2* (7), 548–558. https://doi.org/10.1021/accountsmr.1c00087.
(22) Zhang, L.; Xu, Q.; Hu, Y.; Chen, L.; Jiang, H. Benchmarking the pH–Stability Relationship of Metal Oxide Anodes in Anion Exchange Membrane Water Electrolysis. *ACS Sustainable Chem. Eng.* **2023**, *11* (36), 13251–13259. https://doi.org/10.1021/acssuschemeng.3c01619.
(23) Wu, X.; Chen, N.; Hu, C.; Klok, H.-A.; Lee, Y. M.; Hu, X. Fluorinated Poly(Aryl Piperidinium) Membranes for Anion Exchange Membrane Fuel Cells. *Advanced Materials* **2023**, 2210432. https://doi.org/10.1002/adma.202210432.
(24) Chen, N.; Jiang, Q.; Song, F.; Hu, X. Robust Piperidinium-Enriched Polystyrene Ionomers for Anion Exchange Membrane Fuel Cells and Water Electrolyzers. *ACS Energy Lett.* **2023**, 4043–4051. https://doi.org/10.1021/acsenergylett.3c01402.
(25) Thangavel, P.; Lee, H.; Kong, T.-H.; Kwon, S.; Tayyebi, A.; Lee, J.; Choi, S. M.; Kwon, Y. Immobilizing Low-Cost Metal Nitrides in Electrochemically Reconstructed Platinum Group Metal (PGM)-Free Oxy-(Hydroxides) Surface for Exceptional OER Kinetics in Anion Exchange Membrane Water Electrolysis (Adv. Energy Mater. 6/2023). *Advanced Energy Materials* **2023**, *13* (6), 2370022. https://doi.org/10.1002/aenm.202370022.
(26) Xu, Q.; Oener, S. Z.; Lindquist, G.; Jiang, H.; Li, C.; Boettcher, S. W. Integrated Reference Electrodes in Anion-Exchange-Membrane Electrolyzers: Impact of Stainless-Steel Gas-Diffusion Layers and Internal Mechanical Pressure. *ACS Energy Lett.* **2021**, *6* (2), 305–312. https://doi.org/10.1021/acsenergylett.0c02338.